JPE 18-3-9

https://doi.org/10.6113/JPE.2018.18.3.736
ISSN(Print): 1598-2092 / ISSN(Online): 2093-4718

Robust Time Delay Compensation for DTC-Based Induction Machine Systems via Extended State Observers

Fengxiang Wang*, Junxiao Wang†, and Li Yu**

*Quanzhou Institute of Equipment Manufacturing, Haixi Institute,
Chinese Academy of Sciences, Quanzhou, China
†,**College of Information Engineering, Zhejiang University of Technology, Hangzhou, China

Abstract

This paper presents an extended state observer (ESO) based direct torque control (DTC) for use in induction motor systems to handle the issues of time delays, load torque disturbances and parameter uncertainties. Direct torque control offers an excellent torque response and it does not require a proportion integration (PI) controller in the current loop. However, a PI controller is still adopted in the outer speed loop to generate the torque reference value, which is a slow method. An ESO based compound control scheme is proposed to improve the response rate and accuracy of the torque reference signal, especially when load torque is injected. In addition, the time delay problem is analyzed and compensated for in this paper to reduce torque ripples. The proposed disturbance compensation technique based direct control scheme is shown to have good performance both in the transient and stable states via simulations and experimental results.

Key words: Extended state observer (ESO), Direct torque control (DTC), Induction machine, Time delay

I. INTRODUCTION

During the past few decades, a lot of research efforts have been focused on the control of induction machines. Field Oriented Control (FOC) and DTC are popular control schemes in the industry [1]. The FOC scheme decouples the torque and flux so that induction machines can be controlled independently. Unlike the FOC method, DTC can produce a torque response using the switching vector directly, rather than via a current controller [2]. This makes it modulator and inner current PI controller unnecessary [6]. Thus, the system is easy to be implemented and has fast dynamics. There are some existing DTC schemes [3]-[8] that use a look up table (LUT). Deadbeat DTC and sliding mode DTC are improved methods for reducing torque ripples [11]-[13].

For the traditional ST-DTC scheme, the finite voltage vectors are predefined in a switching-table off-line to change the torque and flux. Based on the generated logic variables using torque and flux hysteresis comparators, the output voltage vector can be decided directly by a pre-stored switching table. However, the hysteresis characteristic of the traditional DTC control scheme has two disadvantages. Firstly, the switching frequency of the inverter is variable and dependent on the values of the hysteresis band. Secondly, the torque ripple is large [3]-[5].

Many improved DTC schemes have been presented to deal with these drawbacks. Direct mean torque control was proposed to deal with hysteresis limits in [4]. It can obtain a constant switching frequency. Band constrained scheme was investigated in [5]. It has been verified to be an effective method. These methods reduce the torque ripple while retaining the standard control structure. Space vector pulse wide modulation (SVPWM) based DTC has also been verified to be a useful solution [9], [15], [18]. It can produce less torque ripples. A multilevel inverter was used to obtain more voltage vectors in [6]. It can also deal with the problem

Manuscript received Oct. 31, 2017; accepted Feb. 3, 2018
Recommended for publication by Associate Editor Gaolin Wang.
†Corresponding Author: wangjunxiao19860128@126.com
Tel: +86-18795895157, Zhejiang University of Technology
*Quanzhou Institute of Equipment Manufacturing, Haixi Institute, Chinese Academy of Sciences, China
**College of Information Eng., Zhejiang University of Technology, China

of torque ripple. These methods can suppress the torque ripple. However, they either increase the system complexity or the hardware cost. Recently, the causes of large ripples for the conventional DTC scheme were analyzed, and a time delay compensated DTC was investigated to reduce ripples [14]. This method can achieve excellent performance. However, it is dependent on the motor parameter values. In addition, parameter uncertainties and load toque also influence the induction machine system control performance [16]-[20].

In recent years, due to the unavoidable influences of external unknown disturbances and system model parameter uncertainties, disturbance estimation based feed-forward compensation methods have been shown to be promising solutions [21]-[24]. The observer design is the main work in different compensation methods. A disturbance observer is proposed in two link robotic manipulator systems [25]. It can observe lumped disturbances and compensate them in the feedforward channel, and it has been verified and applied in PMSM control systems [23]. ESO is another disturbance estimate method [26]. It was developed and originated from active disturbance reject control (ADRC). The lumped disturbances are defined as a new system state, so that the estimated value can be employed to finish the compensation [27]-[28].

In this paper, an ESO based direct control scheme is developed by analyzing the existing time delay problems of DTC based induction machine systems as well as the problems of load disturbances and system parameter perturbations. The main contributions of this paper are shown as follows:

- An ESO technique is used for compensating the time delay problem.
- In addition, by considering the importance of the torque reference, a disturbance based technique is applied in the outer speed control loop.
- Parameter uncertainties are considered in this work. A robust estimation model is used to achieve a good behavior.

The remainder of this paper is organized as follows. The models of an induction machine and a two-level voltage source inverter are introduced in section II. An extended state observer design and an improved direct torque controller are designed in section III. Simulation and experimental results are presented to show the effectiveness of the proposed controller in section IV. Some conclusions are given in section V.

II. Model Description of an Induction Machine and an Inverter

The mathematical model of a squirrel-cage IM can be described as follows.

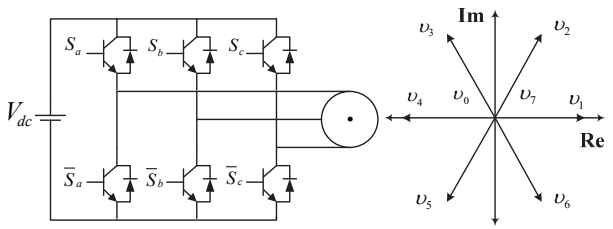

(a) (b)

Fig. 1. Diagrams of: (a) inverter and (b) finite voltage vector.

$$v_s = R_s \cdot i_s + \frac{d}{dt}\psi_s \tag{1}$$

$$0 = R_r \cdot i_r + \frac{d}{dt}\psi_r - j \cdot \omega \cdot \psi_r \tag{2}$$

$$\psi_s = L_s \cdot i_s + L_m \cdot i_r \tag{3}$$

$$\psi_r = L_r \cdot i_r + L_m \cdot i_s \tag{4}$$

$$\frac{d\omega}{dt} = \frac{T_e}{J} - \frac{T_L}{J} - \frac{B\omega}{J} \tag{5}$$

$$T_e = \frac{3}{2} \cdot p \cdot (\psi_s \times i_s) \tag{6}$$

where v_s denotes the stator voltage vector, and ψ_s and ψ_r represent the stator flux and rotor flux, respectively. i_s and i_r are the stator and rotor currents, respectively. R_s and R_r are the stator and rotor resistances, respectively. L_s, L_r and L_m are stator, rotor and mutual inductances, respectively. ω is the mechanical speed. p is the number of pole pairs, and T_L and T_e denote the load torque and electromagnetic torque, respectively. J is the moment of inertia, and B is the friction coefficient.

Fig. 1 shows a two-level voltage source inverter that can produce eight voltage vectors. The switching state vector S can be described as follows:

$$S = \frac{2}{3}(S_a + aS_b + a^2 S_c) \tag{7}$$

where $a = e^{j2\pi/3}$, $S_i = 1$ means that S_i is on and $\bar{S}_i$ is off, and $i = a, b, c$. The voltage v_s is related to the switching state S by:

$$v_s = V_{dc} S \tag{8}$$

Where V_{dc} is the dc link voltage.

III. ESO Based Improver DTC Design

Fig. 2 gives the proposed control diagram description for induction machine systems. The system consists of two parts: an external speed controller and inner torque and flux controllers. An extended state observer is designed to achieve adjustable speed control. Two hysteresis controllers are designed for torque and stator flux magnitude control. A predefined look up table is designed for the switcher selections.

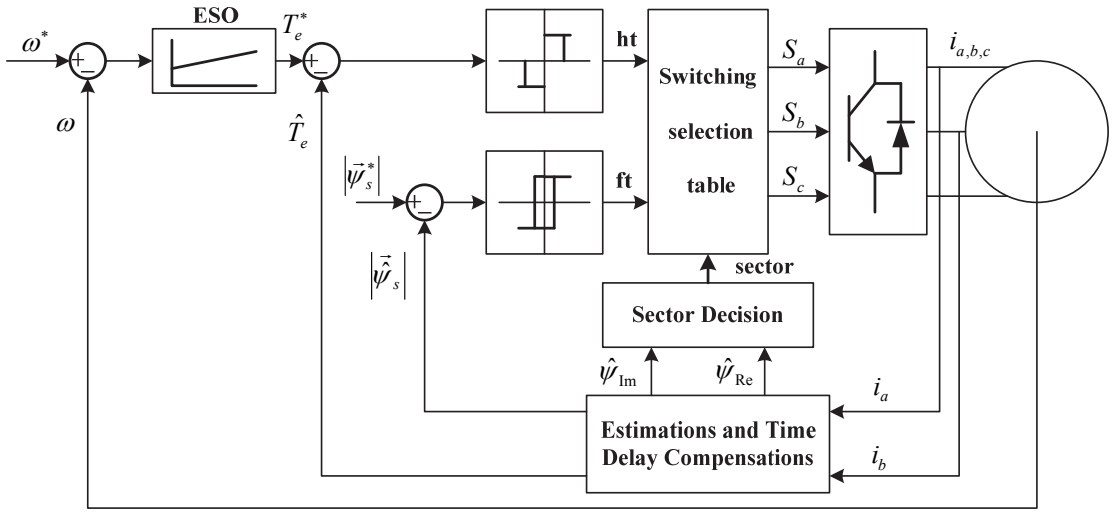

Fig. 2. Block diagram of an extended state observer based direct torque control for induction machine systems.

To obtain a more reasonable sector calculation, improved estimation and time delay compensations are proposed.

A. Extended State Observer

For obtaining the lumped disturbance estimation, which includes unknown load torque and parameter variations, based on Eq. (5), the model can be redefined as $\dot{\omega} = \frac{T_e^*}{J_n} + d_\omega(t)$. Where T_e^* is torque reference, and the lumped disturbance is denoted as $d_\omega(t) = \frac{T_e^*}{J_n} - \frac{T_e}{J} - \frac{T_L}{J} - \frac{B_\omega}{J}$. Using the ESO technique, the disturbance estimation $\hat{d}_\omega(t)$ is designed as:

$$\begin{aligned} \dot{z}_1 &= \frac{T_e^*}{J_n} + z_2 + \beta_1(\omega - z_1) \\ \dot{z}_2 &= \beta_2(\omega - z_1) \end{aligned} \tag{9}$$

where $z_1 = \hat{\omega},\ z_2 = \hat{d}_\omega(t)$ and $\beta_1, \beta_2 > 0$.

Assumption 3.1: For an induction motor system, suppose the lumped disturbances d(t) are constants or bounded in the steady state, i.e., $\lim_{t\to 0} \dot{d}(t) = 0\ or \le l$.

Lemma 3.1: [29] Consider the system $\dot{x} = F(x, \omega)$, where $x(t)$ and ω(t) are the system state and control input. It is input-to-state stable (ISS). If the control input satisfies $\lim_{t\to 0} \omega(t) = 0$, the control system states satisfy $\lim_{t\to 0} x(t) = 0$.

For the observer system of Eqs. (9), define:

$$e_\omega(t) = \omega - z_1 \tag{10}$$

$$e_d(t) = d_\omega(t) - \hat{d}_\omega(t) \tag{11}$$

Substituting Eqs. (10)-(11) into the derivative of $e_\omega(t), e_d(t)$, yields:

$$\dot{e}_\omega(t) = e_d - \beta_1 e_\omega \tag{12}$$

$$\dot{e}_d = \dot{d}_\omega - \beta_2 e_\omega \tag{13}$$

Choosing a Lyapunov function as Eq. (14) yields:

$$V_{e_d} = \frac{1}{2} e_d^2 + \frac{\beta_1}{2} e_\omega^2 \tag{14}$$

where $\beta_1 > 0$.

Taking the time derivative of V_{e_d}, and using Eqs. (12)-(13), the following is obtained:

$$\begin{aligned} \dot{V}_{e_d} &= e_d \dot{e}_d + \beta_2 e_\omega \dot{e}_\omega \\ &= e_d(\dot{d}_\omega - \beta_2 e_\omega) + \beta_2 e_\omega(e_d - \beta_1 e_\omega) \\ &= -\beta_1 \beta_2 e_\omega^2 + e_{d_1} \dot{d}_\omega \end{aligned} \tag{15}$$

If the lumped disturbance satisfies Assumption 3.1, the error system (12)-(13) satisfies ISS. It should noted that $\lim_{t\to 0} \dot{d}_\omega(t) = 0$, according to Lemma 3.1. Then it yields $\lim_{t\to 0} e_d(t) = 0$, $\lim_{t\to 0} e_\omega(t) = 0$, where $\beta_1, \beta_2 > 0$, and the errors in Eqs. (12)-(13) are driven to the desired equilibrium point asymptotically.

B. Flux Observers

For the ESO-DTC control structure described in Fig. 2, the stator flux $\hat{\psi}_s(k+1)$, rotor flux $\hat{\psi}_r(k+1)$ and electromagnetic torque $\hat{T}_e(k+1)$ should be obtained. Considering the system parameter uncertainties, the extended state observer is also designed to improve system robustness. Using stator current information, the flux observers can be designed as follows:

$$\frac{d}{dt}\psi_s = v_s - R_s \cdot i_s \tag{16}$$

$$\psi_r = \frac{L_r}{L_m}(\psi_s - \frac{L_s L_r - L_m^2}{L_r} i_s) \tag{17}$$

Combining Eqs. (2)-(4), the rotor flux observer is designed as (18).

$$\frac{d}{dt}\hat{\psi}_r = \frac{L_m R_r}{L_r}\cdot i_s - (\frac{R_r}{L_r} - j\cdot\omega)\cdot\hat{\psi}_r + K_{\psi_{rp}}(\psi_r - \hat{\psi}_r) + \hat{d}_{\psi_r} \quad (18)$$

$$\dot{\hat{d}}_{\psi_r} = K_{\psi_{ri}}(\psi_r - \hat{\psi}_r) \quad (19)$$

C. Time Delay Compensation

In the ideal condition, as shown in Fig. 3, stator current information is obtained by sensors at the discrete instant k. At the same time, the selected switching vector $S(k)$ is applied for driving the machine via an inverter. Notice that the practical microprocessor needs one period to calculate the current value, execute the algorithm and produce the final switching state, with a one cycle delay. Thus, the final control signal is given to the inverter nearly at the time step $k+1$ in reality, and not at the time step k as in the simulation.

To compensate this time delay issue for the traditional DTC method, a compensation scheme is considered and described in Fig. 3.

The final controller output of the voltage vector $\vec{v}_s(k)$ at the time $k+1$ is used based on the stator current, stator flux and torque at time $k+1$. Therefore, the proposed control strategy is time-consistent. The stator current observer is designed as follows:

$$\dot{\hat{i}}_s = -\frac{L_m^2 R_r}{(L_m^2 - L_r L_s)L_r}\cdot i_s + \frac{L_r}{L_m^2 - L_r L_s}R_s\cdot i_s - \frac{L_r}{L_m^2 - L_r L_s}\cdot v_s - \frac{L_m}{L_m^2 - L_r L_s}(\frac{R_r}{L_r - j\omega})\cdot\hat{\psi}_r\hat{d}_{i_s} + K_{i_{sp}}\cdot(i_s - \hat{i}_s) \quad (20)$$

$$\dot{\hat{d}}_{i_s} = K_{i_{si}}\cdot(i_s - \hat{i}_s) \quad (21)$$

the discrete time stator current observer is designed as follows:

$$\hat{i}_s(k+1) = (1 - \frac{T_s L_m^2 R_r}{(L_m^2 - L_r L_s)L_r})\cdot\hat{i}_s(k) + \frac{T_s L_r}{L_m^2 - L_r L_s}R_s\cdot\hat{i}_s(k) - \frac{T_s L_r}{L_m^2 - L_r L_s}\cdot v_s(k) - \frac{T_s L_m}{L_m^2 - L_r L_s}(\frac{R_r}{L_r - j\omega})\cdot\hat{\psi}_r(k)\hat{d}_{i_s}(k) + K_{i_{sp}}\cdot(i_s(k) - \hat{i}_s(k)) \quad (22)$$

$$\hat{d}_{i_s}(k+1) = \hat{d}_{i_s}(k) + T_s\cdot K_{i_{si}}\cdot(i_s(k) - \hat{i}_s(k)) \quad (23)$$

where T_s is the control period. The stability analysis of Eqs. (16)-(23) is similar to the above proof.

D. Improved Direct Torque Controller Design

The important part of the ESO-DTC is to design hysteresis controllers for regulating the stator flux and electromagnetic torque. Under the hysteresis controller output, the inverter switching control signal can be selected from a pre-stored LUT. In this control scheme, two assumptions must be considered. Firstly, suppose that the stator resistance voltage drop can be ignored in the stator voltage equation (1). Thus, the stator flux can be expressed by the employed inverter voltage vector in one sampling interval as follows:

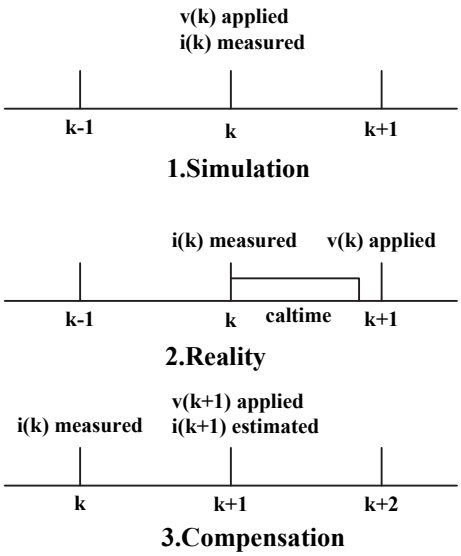

Fig. 3. Time delay compensation.

$$\Delta\vec{\psi}_s \approx \vec{v}_s\cdot T_s \quad (24)$$

where T_s is the sampling time.

The electromagnetic torque in the ESO-DTC can be expressed as:

$$T_e = \frac{2}{3}\cdot\frac{L_m}{\sigma\cdot L_s\cdot L_r}\cdot p\cdot|\vec{\psi}_r|\cdot|\vec{\psi}_s|\cdot\sin(\delta) \quad (25)$$

Aiming to obtain electromagnetic torque, the relationship between the flux and the angle can be obtained. Secondly, suppose that the rotor flux response is slower than the response of the stator flux. Then the rotor flux can be considered as invariant during one sampling interval. Therefore, the electromagnetic torque can be changed by tuning the stator flux angle based on the proper voltage vector.

Under these assumptions, the electromagnetic torque and stator flux magnitude can be controlled. The ESO-DTC control structure is described in Fig. 2. The stator flux and angle are calculated from the voltage equation and measured current. The electromagnetic torque estimation is obtained based on the stator flux and rotor flux estimation. The errors of the electromagnetic torque and flux are fed to the hysteresis controllers where the hysteresis bands are ht and ft respectively. Then the switching signal can be decided via a predefined LUT for driving the inverter based induction machine.

The desired flux value is set to be constant. The torque reference signal is generated by the speed loop, and it is fed

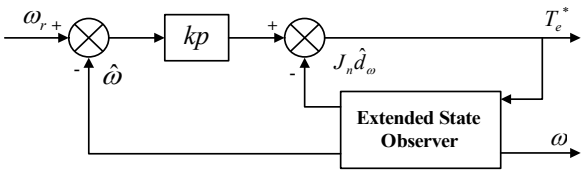

Fig. 4. Compensation method based on an extended state observer.

to the hysteresis-based torque controller. Based on the disturbance estimation, the electromagnetic torque reference T_e^* could be designed by Eq. (26).

$$T_e^* = k_p(\omega_r - \hat{\omega}) - J_n\hat{d}_\omega \tag{26}$$

which is produced by the ESO-based controller shown as Fig. 4, where ω_r denotes the speed reference. The speed estimation $\hat{\omega}$ and the disturbance estimation $\hat{d}_\omega$ are obtained by the states z_1 and z_2 in the ESO (9). Unlike a PI feedback controller, the integral item is eliminated by a feed-forward scheme which can improve the disturbance rejection ability.

Remark 3.1. Because the load torque is unknown, the integral term can compensate them. However, it is a slow manner. Like the deadbeat-like idea, if the lumped torque disturbances is soft measured or estimated, the torque reference can be generated quickly. The propose control scheme is motivated by this idea. In addition, the time delay problem is analyzed, and the torque ripple is clearly reduced by the proposed compensation. This is another contribution of this paper.

IV. Simulation and Experimental Results

Performance tests of the DTC based method (ESO-DTC) are verified by numerical simulations and experiments. The parameters of the induction machine in this self-constructed bench are shown in Table I.

A. Simulation Results

Simulation results using the MATLAB/Simulink tool are presented. The main motor parameter values are given in Table I. They are calculated by experimental tests. The speed reference is $\omega_r = 12000/(2*\pi)rpm$.

In order to show the effectiveness of the novel ESO-DTC method proposed in this paper, based on the mathematical model and simulation environment, the conditions of the torque load disturbance and inertia value varying are considered for the performance verification.

Firstly, to determine the disturbance rejection capability of the proposed ESO-DTC method, simulation results are presented, considering load torque variations. From Fig. 6(a), it can be seen that the speed response is good when the load torque is given suddenly.

In addition, for testing the robustness, the inertia value is also varying. From Fig. 6(b), it can be seen that the flux and torque speed responses are also insured, even if the inertia value is varied to 20 J_{nom}.

TABLE I
Controlled IM Parameter Values

Descriptions	Parameters	Nominal Values
DC link Voltage	V_{dc}	582(V)
Stator Resistance	R_s	2.68Ω
Rotor Resistance	R_r	2.13Ω
Inductance	L_m	275.1(mH)
Stator Inductance	L_s	283.4(mH)
Rotor Inductance	L_r	283.4(mH)
Pole Pairs	P	1.0
Speed	ω_{nom}	2772.0(RPM)
Torque	T_{nom}	7.5(Nm)
Inertia	J	0.005Kg · m^2

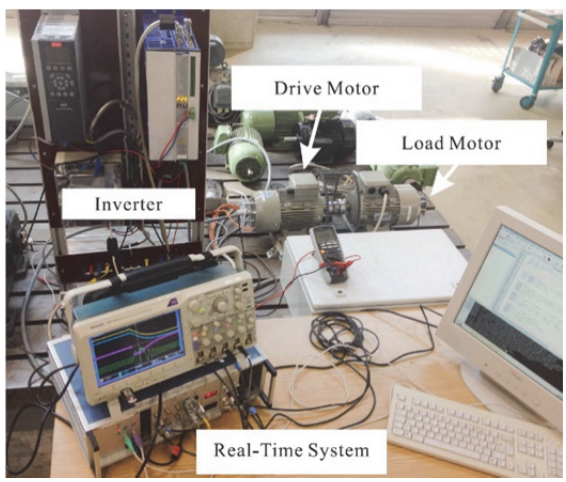

Fig. 5. Photo of the test bench.

B. Experimental Discussion

The ESO-DTC method has been implemented on an experimental setup. It includes two 2.2 kW squirrel-cage IMs. The load machine is controlled by a Danfoss VLT FC-302 3.0-kW inverter. It is used for loading torque. The other machine is controlled by a self-modified SERVOSTAR620 14-kVA inverter based self-made 1.4 GHz real-time computer system. The rotor position and speed information are measured and calculated by a 1024-point incremental encoder. The parameters of the induction motor are given in Table I. Fig. 5 shows the test bench in detail.

The system performance during the reversal process with speed range changes from 2720 rpm to -2720 rpm and then back to 2720 rpm is tested. The responses of the speed, electromagnetic torque and stator current are described in Fig. 7. During the response process, the electromagnetic torque reaches its saturation value at 7.5Nm at the initial time. The stator flux magnitude value is 0.71Wb during the speed reverse dynamic process. It is measured in the computer based on the current and voltage information. The flux ripple is less than 0.05Wb in the whole range, which is also acceptable.

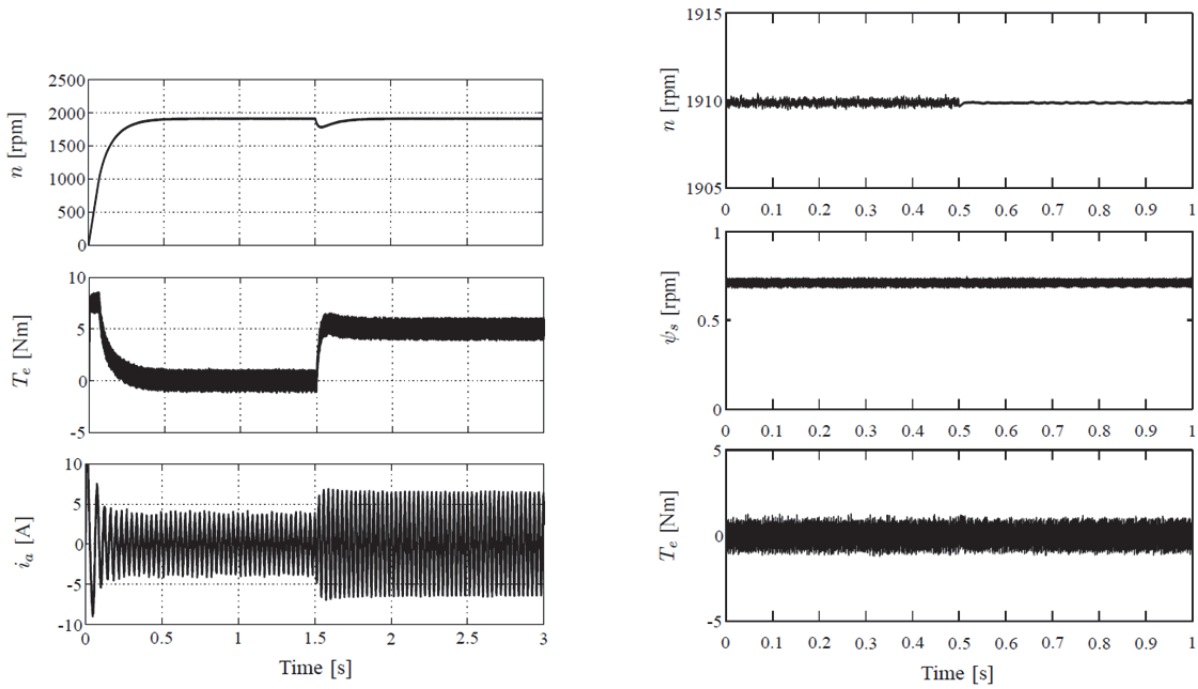

Fig. 6. Speed, torque, stator current and flux responses when the desired speed is $\omega_r = 12000/(2 * \pi) rpm$. (a) Load torque given at 5Nm. (b) Load torque given at 5Nm.

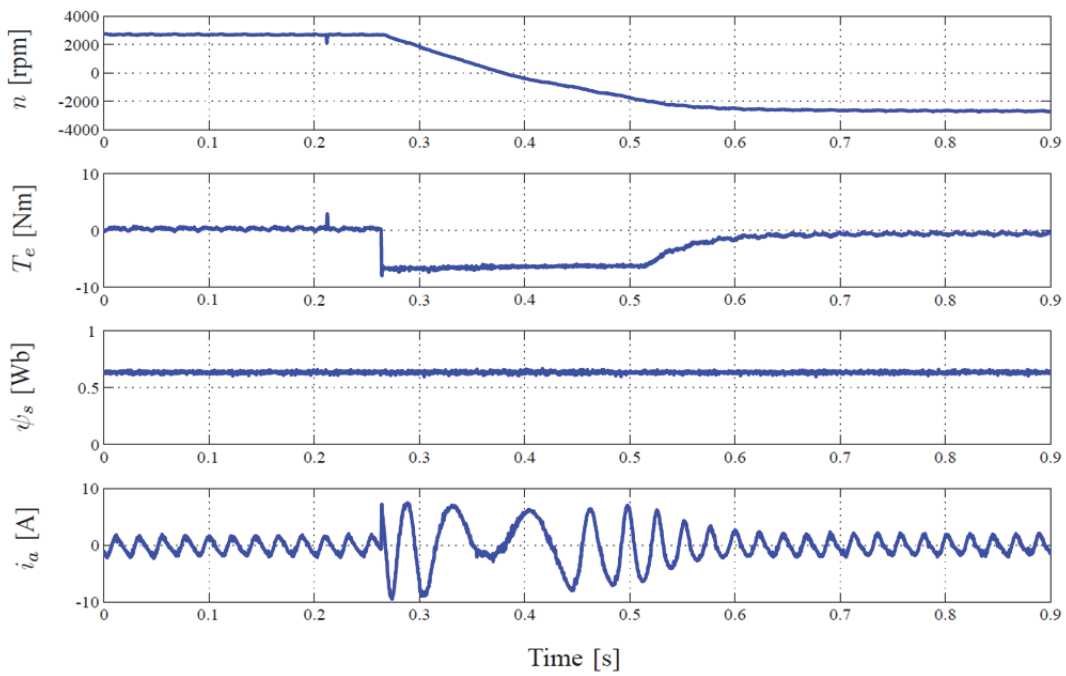

Fig. 7. Speed (2720 rpm to -2720 rpm), torque, stator flux and stator current responses.

Figs. 8(a)-8(c) show the good behaviors at the steady state, including the speed, torque, current and stator flux in the stator reference frame. As shown in Fig. 8(a), it can be concluded that the disturbance rejection performance is also ensured when the rated speed is 400 rpm and that the load torque is given at 5Nm. Thus, the extended state observer and DTC method are completely incorporated. The torque ripple is about 1.0 Nm.

A torque dynamics test has been carried out for showing the torque step performance. As described in Fig. 9(a), the desired torque is changed from 0 Nm to the rated value of 7.5 Nm, which is produced by the proposed controller. The

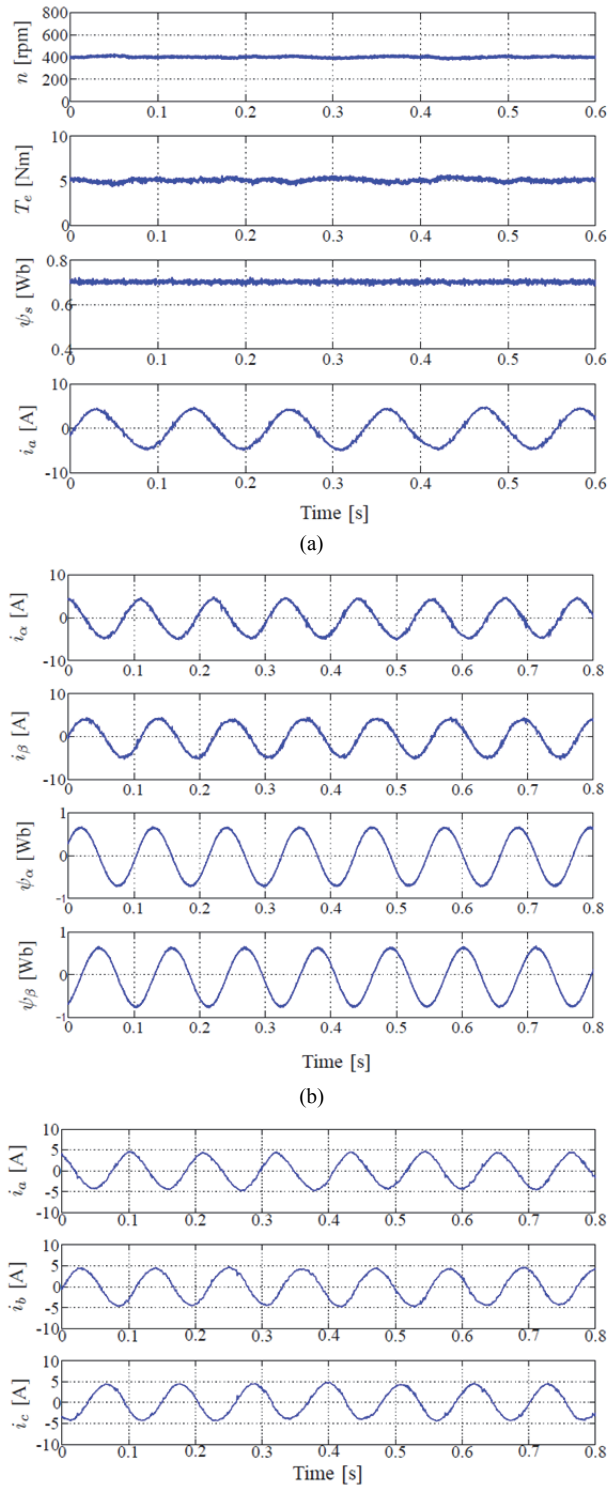

Fig. 8. Speed (400rpm), torque (5Nm), stator flux and stator current responses.

torque ripple is less than 2 Nm and the settling time is about 400μs. This fast torque response is one advantage of the proposed ESO based DTC control scheme. It should be noticed that the torque reference looks faster than the load torque response, since it is generated by a load machine with

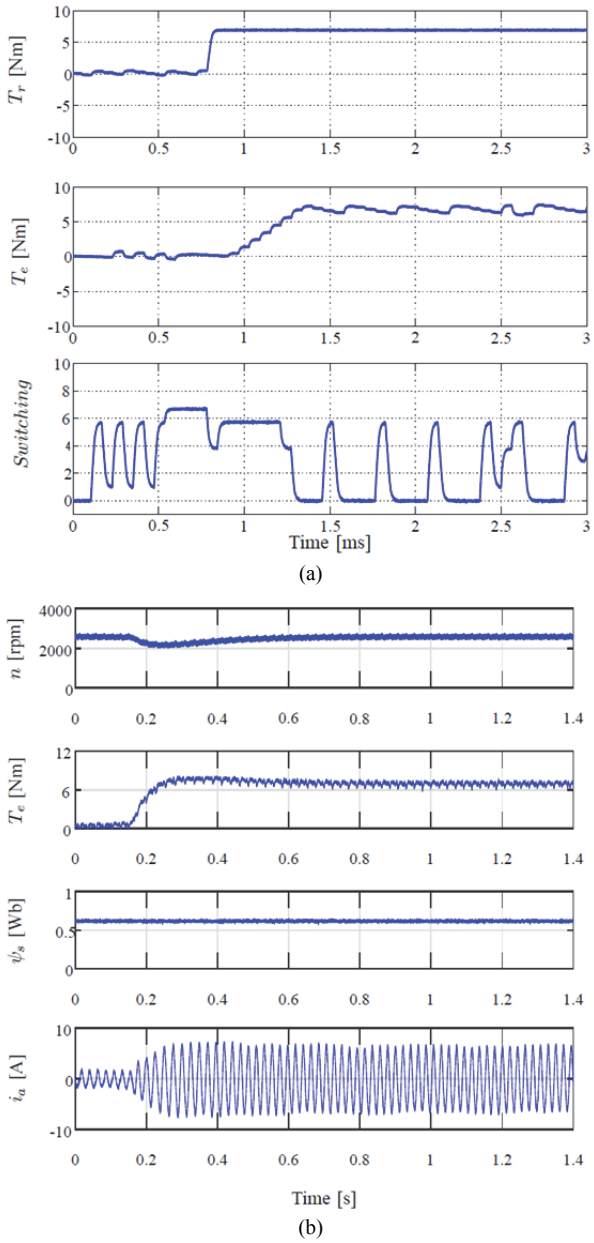

Fig. 9. (a) Torque reference (7.5 Nm), torque and switching signal responses; (b) Speed (2720 rpm), torque, stator flux and stator current responses.

a commercial inverter. Fig. 9(b) shows that the system is stable when it is given at a full load torque suddenly. The rated speed is set at 2772rpm. A sudden load change (from 0Nm to 7.5Nm) is given at 0.185s. The speed recovery process only need 0.28s.

From Figs. 10(a)-10(b), when the inertia value J and R_s are time varying, the system is also stable until J=20J_{nom} and R_s, which is changed from 2.4Ω and 4.7Ω. The system robustness is good. In addition, from Figs. 11(a)-11(b), it is easy to find that the proposed time delay compensation method has less torque ripple than without the compensation. This is the important contribution of the proposed method.

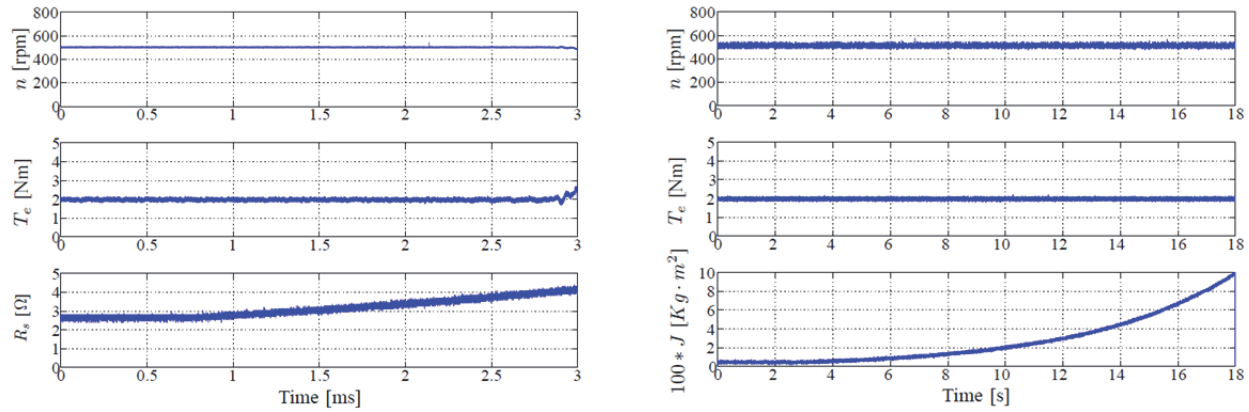

(a) (b)

Fig. 10. Speed (500 rpm), torque, stator resistance and inertia value waveforms. (a) Stator resistance is varying, (b) Inertia value is varying.

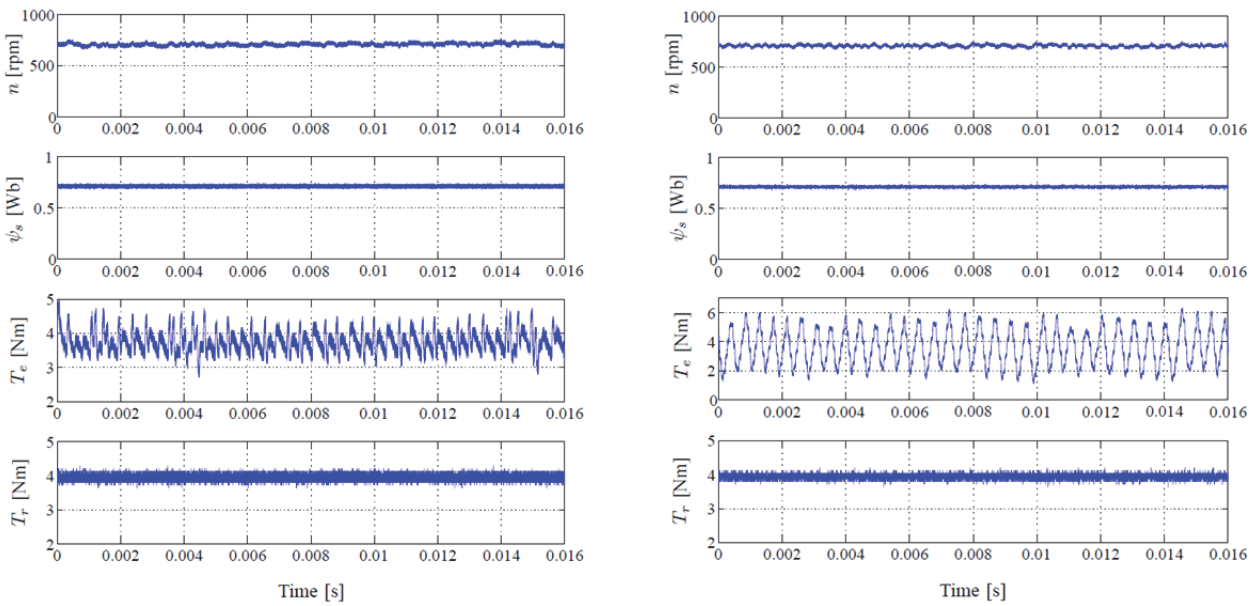

(a) (b)

Fig. 11. Speed (750 rpm), flux, torque and torque reference responses (4Nm). (a) Proposed method (ESO-DTC), (b) Without compensation (DTC).

V. Conclusion

In this paper, an extended state observer based direct control method is proposed. The torque reference is generated by a direct method via disturbance compensation theory. The problems of time delays, parameter variations and load disturbances are considered in the controller design. By using the ESO method, the model of the estimation of the torque and flux are compensated. Therefore, good robustness is obtained at both the transient and stable states.

Acknowledgment

This work was supported by the National Natural Science Foundation of China under Grant No.51507172 and No.U1709213.

References

[1] G. Buja and M. Kazmierkowski. “Direct torque control of PWM inverter-fed AC motors-a survey,” *IEEE Trans. Ind. Electron*., Vol. 51, No. 4, pp. 744-757, Aug. 2004.

[2] K. Wang, R. D. Lorenz, and N. A. Baloch, “Improvement of back-EMF self-sensing for induction machines when using deadbeat-direct torque and flux control,” *IEEE Trans. Ind. Appl*., Vol. 53, No. 5, pp. 4569-4578, Sep./Oct. 2017.

[3] C. Xia, J. Zhao, Y. Yan, and T. Shi, “A novel direct torque control of matrix converter-fed PMSM drives using duty cycle control for torque ripple reduction,” *IEEE Trans. Ind. Electron.*, Vol. 61, No. 1, pp. 2700-2713, Jun. 2014.

[4] A. K. Mishra, B. S. Rajpurohit, and R. Kumar, “Induction machine drive design for enhanced torque profile,” *IEEE Trans. Ind. Appl*., Vol.54, No. 2, pp. 1283-1291, Mar./Apr. 2018.

[5] V. Ambrozic, G. Buja, and R. Menis, "Band-constrained technique for direct torque control of induction motor," *IEEE Trans. Ind. Electron*., Vol. 51, No. 4, pp. 776-784, Aug. 2004.
[6] Y. Zhang, J. Zhu, Z. Zhao, W. Xu, and D. G. Dorrell, "An improved direct torque control for three-level inverter-fed induction motor sensorless drive," *IEEE Trans. Power Electron*., Vol. 27, No. 3, pp. 1502-1513, Mar. 2012.
[7] C. Lascu, I. Boldea, and F. Blaabjerg, "Variable-structure direct torque control-a class of fast and robust controllers for induction machine drives," *IEEE Trans. Ind. Electron*., Vol. 51, No. 4, pp. 785-792, Aug. 2004.
[8] C. Lascu, I. Boldea, and F. Blaabjerg, "Direct torque control of sensorless induction motor drives: a sliding-mode approach," *IEEE Trans. Ind. Electron*., Vol. 40, No. 2, pp. 582-590, Mar. 2004.
[9] D. Casadei, F. Profumo, G. Serra, and A. Tani, "FOC and DTC: Two viable schemes for induction motors torque control," *IEEE Trans. Ind. Electron*., Vol. 17, No. 5, pp. 779-787, Sep. 2002.
[10] B. Kenny and R. Lorenz, "Stator and rotor-flux-based deadbeat direct torque control of induction machines," *IEEE Trans. Ind. Appl*., Vol. 39, No. 4, pp. 1093-1101, Jul./Aug. 2003.
[11] G. Wang, J. Qi, J. Xu, X. Zhang, and D. Xu, "Antirollback control for gearless elevator traction machines adopting offset-free model predictive control strategy," *IEEE Trans. Ind. Electron*., Vol. 62, No. 10, pp. 6194-6203, Oct. 2015.
[12] Z Yin, Y Zhang, C Du, J. Liu, X. Sun, and Y. Zhong, "Research on anti-error performance of speed and flux estimation for induction motors based on robust adaptive state observer," *IEEE Trans. Ind. Electron*., Vol. 63, No. 6, pp. 3499-3510, 2016.
[13] Q. Zhu, Z. Yin, Y. Zhang, J. Niu, Y. Li, and Y. Zhong, "Research on two-degree-of-freedom internal model control strategy for induction motor based on immune algorithm," *IEEE Trans. Ind. Electron*., Vol. 63, No. 6, pp. 1981-1992, Mar. 2016.
[14] J. Beerten, J. Verveckken, and J. Driesen, "Predictive direct torque control for flux and torque ripple reduction," *IEEE Trans. Ind. Electron.*, Vol. 57, No. 1, pp. 404-412, Jan. 2010.
[15] G. S. Buja and M. P. Kazmierkowski, "Direct torque control of PWM inverter-fed AC motors-A survey," *IEEE Trans. Ind. Electron*., Vol. 51, No. 4, pp. 744-757, Aug. 2004.
[16] T. Geyer, "Model predictive direct torque control: derivation and analysis of the state-feedback control law," *IEEE Trans. Ind. Appl*., Vol. 49, No.5, pp. 2146-2157, Sep. 2013.
[17] K. B. Lee, F. Blaabjerg, and T. W. Yoon. "Speed-sensorless dtc-svm for matrix converter drives with simple nonlinearity compensation," *IEEE Trans. Ind. Appl*., Vol. 43, No. 6, pp. 1639-1649, 2007.
[18] S. Kouro, R. Bernal, H. Miranda, C. Silva, and J. Rodriguez, "High-performance torque and flux control for multilevel inverter fed induction motors," *IEEE Trans. Power Electron*., Vol. 22, No. 6, pp. 2116-2123, Nov. 2007.
[19] J. Rodriguez, P. Cortes. Predictive control of power converters and electrical drives, 1st ed. Wiley-IEEE Press, 2012.
[20] Z. Xu and M. Rahman, "Comparison of a sliding observer and a kalman filter for direct-torque-controlled IPM synchronous motor drives," *IEEE Trans. Ind. Electron*., Vol. 59, No. 11, pp. 4179-4188, Nov. 2012.
[21] S. Yin and B. Xiao, "Tracking control of surface ships with disturbance and uncertainties rejection capability," *IEEE/ASME Trans. Mechatron*., Vol. 22, No. 3, pp. 1154-1162, Jun. 2017.
[22] H. Liu and S. Li. "Speed control for PMSM servo system using predictive functional control and extended state observer," *IEEE Trans. Ind. Electron*., Vol. 59, No. 2, pp. 1171-1183, Feb. 2012.
[23] W. Chen, "Disturbance observer based control for nonlinear systems," *IEEE/ASME Trans. Mechatronic*., Vol. 9, No. 4, pp. 706-710, Dec. 2004.
[24] S. Li, J. Yang, W. Chen, and X. Chen. Disturbance Observer-Based Control: Methods and Applications, CRC press, 2014.
[25] M. Nakao, K. Ohnishi, K. Miyachi. "Robust decentralized joint control based on interference estimation," in *Robotics and Automation, 1987 IEEE International Conference on*, Vol. 4, pp. 326-331, 1987.
[26] J. Han, "From PID to active disturbance rejection control," *IEEE Trans. Ind. Electron.*, Vol. 56, No. 3, pp. 900-906, Mar. 2009.
[27] F. Mwasilu, H. Nguyen, H. Choi, and J.-W. Jung, "Finite set model predictive control of Interior PM Synchronous motor drives with an external disturbance rejection technique," *IEEE/ASME Trans. Mechatron*., Vol. 22, No. 2, pp. 762-773, Apr. 2017.
[28] J. Yao, Z. Jiao, and D. Ma, "Extended-state-observer-based output feedback nonlinear robust control of hydraulic systems with backstepping," *IEEE/ASME Trans. Mechatron.*, Vol. 61, No. 11, pp. 6285-6293, Nov. 2014.
[29] H. Khail, *Nonlinear Systems*, 3rd ed. Upper Saddle River, NJ, USA: Prentice-Hall, 2002.

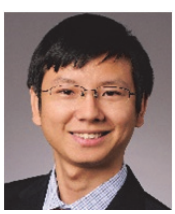

Fengxiang Wang was born in Jiujiang, China, in 1982. He received his B.S. degree in Electronic Engineering and his M.S. degree in Automation from Nanchang Hangkong University, Nanchang, China, in 2005 and 2008, respectively. He received his Ph.D. degree from the Institute for Electrical Drive Systems and Power Electronics, Technische Universitaet Muenchen, Munich, Germany, in 2014. He is presently working at the Haixi Institute, Chinese Academy of Sciences, Quanzhou, China. His current research interests include predictive control and sensorless control for electrical drives.

Junxiao Wang was born in Wuxue, Hubei Province, China, in 1986. He received his B.S. and M.S. degrees in Control Theory and Control Engineering from the Information Engineering College of the Henan University of Science and Technology (HAUST), Luoyang, China, in 2008 and 2011, respectively. He received his Ph.D.

degree in Control Theory and Control Engineering from the School of Automation, Southeast University (SEU), Nanjing, China, in 2017. He was a visiting Ph.D. student in the Institute for Electrical Drive Systems and Power Electronics at the Technical University of Munich (TUM), Munich, Germany, from September 2015 to September 2016. He is presently working in the College of Information Engineering, Zhejiang University of Technology, Hangzhou, China. His current research interests include advanced control theory and its application to power electronics and AC motor control systems. He was a recipient of the IET Premium Award from the IET Control Theory and Application, in 2017.

Li Yu received his B.S. degree in Control Theory from Nankai University, Tianjin, China, in 1982; and his M.S. and Ph.D. degrees from Zhejiang University, Hangzhou, China. He is presently working as a Professor in the College of Information Engineering, Zhejiang University of Technology, Hangzhou, China. He has authored or co-authored three books and over 200 journal or conference papers. His current research interests include wireless sensor networks, networked control systems and motion control.